

Compressor Design Method in the Supercritical CO₂ Applications

Alireza Ameli*
Laboratory of fluid dynamics
Lappeenranta University of Technology
Lappeenranta, Finland

Aki Grönman
Laboratory of fluid dynamics
Lappeenranta University of Technology
Lappeenranta, Finland

Teemu Turunen-Saaresti
Laboratory of fluid dynamics
Lappeenranta University of Technology
Lappeenranta, Finland

Jari Backman
Laboratory of fluid dynamics
Lappeenranta University of Technology
Lappeenranta, Finland

ABSTRACT

The supercritical CO₂ Brayton cycle has been recently attracting more attention compared to other common energy conversion cycles, chiefly due to its higher thermal efficiency with the relatively low temperature at the turbine inlet compared to its conventional counterparts. Centrifugal compressor operating conditions in the supercritical Brayton cycle are preferably located near the critical point to get advantage of low compressibility factor and eventually low compressor work. In this paper, the design of the compressor using the enthalpy loss models in the supercritical CO₂ region is investigated and the accuracy of the loss models near the critical using real gas is validated. Due to high density of the working fluid near the critical point, compressor size is relatively small. It is noticed that, the friction loss plays a significant role among all loss sources. Therefore, more attention is paid on the skin friction loss and friction coefficient estimations. Results are compared to the experimental measurements conducted at Sandia National Laboratories.

INTRODUCTION

Recently, there has been significant growing interest in the supercritical CO₂ (sCO₂) Brayton cycle as an alternative power conversion cycle, due to the relatively low maximum cycle temperature, high thermal efficiency and compactness. Chiefly due to high density and low specific volume of the fluid in the vicinity of the critical point, turbomachines and heat exchangers are compact compared to other Brayton cycles with different operating conditions [1]. According to a study by Angelino [2], the compressor operating condition near the critical point would improve the compressor performance and consequently cycle efficiency. Despite the enormous benefits of designing compressor in the proximity of the critical point, abrupt behavior of the thermophysical properties makes the design and simulation complicated. Figure 1 depicts the isobaric specific heat capacity variations near the critical point. Quite a few researchers have addressed the turbomachinery simulation and design challenges in the vicinity of the critical point [3]–[10]. One of the most used turbomachinery sizing methods is using the specific speed and specific diameter, $n_s - d_s$, diagram proposed by Balje [11]. However,

* Corresponding author. alireza.ameli@lut.fi

the predicted performance using the $n_s - d_s$ diagram in the supercritical region is imprecise due to real gas approximation and inconsistent behavior of thermodynamics properties [12]; consequently, a meticulous approach is needed to predict compressor performance through the one-dimensional analysis and computational fluid dynamic (CFD).

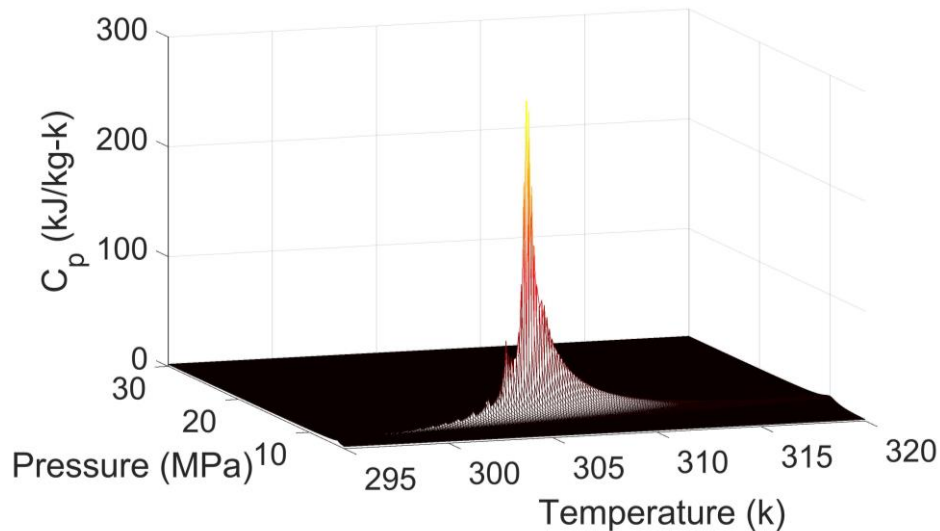


Figure 1. Isobaric specific heat capacity variation near the critical point.

Many researchers have developed loss models for turbomachinery design such as Conrad et al. [13], Coppage et al. [14], Jansen [15], Aungier [16] and Rodgers [17]. Implementing the individual enthalpy loss models into the one dimensional design code was evaluated by Lee et al. [12] in the supercritical region; It was concluded that the future development of loss models are crucial to achieve more trustable designs.

In this paper, the authors have attempted to design and simulate the centrifugal compressor based on the individual enthalpy loss models. Due to the small size of the compressor, because of high density near the critical point, skin friction loss is found to play a noticeable role among the internal enthalpy loss models. To shed more light on this matter, the different skin friction loss models are compared and a general correlation for the skin friction loss and the skin friction factor are derived. Validation and verification have been carried out against the experimental measurements from the Sandia laboratory and time-dependent CFD simulations.

2. METHODOLOGY

The most practical and acceptable accuracy set of enthalpy loss models collected by Oh et al. [18] has been implemented in the in-house mean line code (AIFa CCD [19]) to design and evaluate centrifugal compressor performance. The studied set of loss models were evaluated in the supercritical applications previously [12] [18] [20].

Although, in all studied cases based on the loss models, skin friction factor has been assumed constant, or it has been calculated based on the pipe flow correlations. In the AIFa CCD code, the authors attempt to focus on the friction loss and derive a general correlation with acceptable accuracy for the near critical point applications.

Fluid properties have been derived from the NIST Reference Fluid Thermodynamic and Transport Properties Database 9.1 (REFPROP) [21] based on the Span and Wagner equation of state (SW EOS) model [22]. SW EOS covers the CO₂ thermophysical properties from the triple point up to 1100 K and 800 MPa for temperature and pressure, respectively. This model has been employed and validated by considerable number of researchers in the near critical point applications and is been known as the most accurate EOS especially for CO₂ in the supercritical region [8], [23]–[31].

2.1. MEAN LINE DESIGN

The inlet stagnation conditions, the mass flow rate, the rotor rotational speed and the inlet flow angle are the input variables. The velocity triangle definitions used in the study are illustrated in the figure 2.

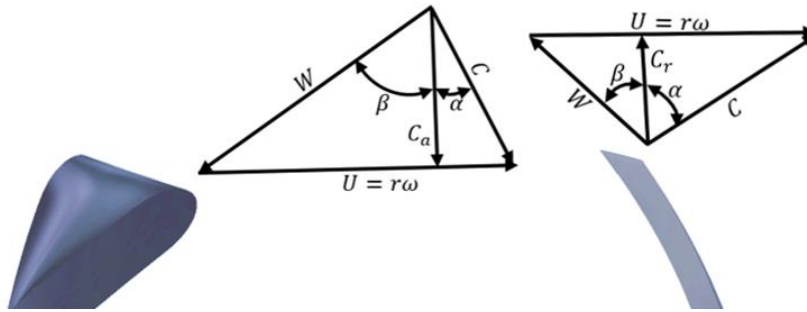


Figure 2. Velocity triangle definitions at the leading (left) and trailing (right) edges.

The centrifugal compressor design is based on the two well-founded equations, Euler and continuity, as follows:

$$(1) h_{t_2} - h_{t_1} = U_2 C_{w_2} - U_1 C_{w_1}$$

$$(2) \dot{m} = \rho A C_{a_1}$$

Where subscripts 1 and 2 stand for the inlet and outlet of the impeller, respectively. In the design code, velocity triangles are calculated at three different radiuses: hub, mean line and the shroud. Mean line radius is estimated as follows

$$(3) r_m = \sqrt{0.5(r_s^2 + r_h^2)}$$

After calculating the velocity triangles at the mentioned locations by using the fluid properties derived from REFPROP, enthalpy loss models are estimated to update the compressor performance parameters.

The set of studied loss models can be classified into internal and external (parasitic) losses. Internal losses consist of incidence, blade loading, skin friction, tip clearance and mixing losses. After updating the compressor performance by considering the internal loss models, external loss models are calculated to take account the extra work of the rotor rotation. External losses are the leakage, the recirculation and the disc friction losses. Enthalpy loss models collected by Oh et al. [18] are summarized in table 1.

Table 1. Individual enthalpy loss models collected by Oh et al. [18].

Loss model	Reference
Incidence loss	Conrad et al. [13]
Blade loading loss	Coppage et al. [14]
Skin friction loss	Jansen [15]
Tip clearance loss	Jansen [15]
Mixing loss	Johnston and Dean [32]
Leakage loss	Aungier [16]
Recirculation loss	Oh et al. [18]
Disc friction loss	Daily and Nece [33]

Details about the individual loss models can be found in the literature. In this study, only the details of skin friction loss and skin friction coefficient are investigating extensively. The skin friction loss occurs due to the viscous shear forces in the boundary layers at walls inside the impeller. The model proposed by Jansen [15] is defined as

$$(4) \Delta h_{SF} = 2C_f \frac{L_b}{d_{hb}} \bar{W}^2,$$

$$\bar{W} = \frac{(2W_2 + W_{1t} + W_{1h})}{4}$$

where \bar{W} stands for the mean relative velocity through the passage, d_{hb} is the average hydraulic diameter of the blade passage and C_f is the skin friction coefficient. The flow path length, L_b is estimated as

$$(5) L_b = \frac{\pi}{8} \left[d_2 - \frac{d_{1t} + d_{1h}}{2} - b_2 + 2L_z \right] \left(\frac{4}{\cos\beta_{1t} + \cos\beta_{1h} + 2\cos\beta_2} \right)$$

and the axial length of the rotor, L_z is estimated by the modeled proposed by Aungier [16] as

$$(6) L_z = d_2 \left(0.014 + \frac{0.023d_2}{d_{1h}} + 1.58\phi \right).$$

Where ϕ stands for flow coefficient. In order to calculate the skin friction factor, C_f , Jansen [15] proposed a correlation which is based on the pipe flow friction calculation as follows

$$(7) c_f = 0.0412(Re)^{-0.1925}$$

$$(8) Re = \frac{\bar{p}\bar{W}d_{hb}}{\bar{\mu}}$$

and the averaged hydraulic diameter of the rotor blade passage d_{hb} as follows

$$(9) d_{hb} = d_2 \left(\frac{\cos\beta_2}{\left[\frac{Z}{\pi} + \frac{d_2 \cos\beta_2}{b_2} \right]} + \frac{0.5 \left(\frac{d_{s1} + d_{h1}}{d_2} \right) \left(\frac{\cos\beta_{s1} + \cos\beta_{h1}}{2} \right)}{\frac{Z}{\pi} + \left(\frac{d_{s1} + d_{h1}}{d_{s1} - d_{h1}} \right) \left(\frac{\cos\beta_{s1} + \cos\beta_{h1}}{2} \right)} \right).$$

Calculating the skin friction factor based on the pipe flow approximations may underestimate the actual value of friction loss due to curved shape of the blade passage. As suggested by Jansen [15], an average value of 0.006 results in a good agreement with the experimental data for the air compressors. However, due to the abrupt behavior of the viscosity and density in the vicinity of the critical point, employing this averaged value should be examined scrupulously.

Another well-established model for the skin friction factor in the turbulence flows was introduced by Schlichting [34] as follows

$$(10) \quad \frac{1}{\sqrt{4c_{f_r}}} = -2 \log \left[\frac{e}{3.71d} \right]$$

$$(11) \quad \frac{1}{\sqrt{4c_{f_s}}} = -2 \log \left[\frac{2.51}{Re_{hb} \sqrt{4c_{f_s}}} \right]$$

Where e stands for the peak to valley surface roughness. c_{f_s} and c_{f_r} stand for the skin friction factors for fully smooth and rough surfaces, respectively. Centrifugal compressors operate in a wide range of the operating conditions, therefore a general statement for the skin friction loss and the skin friction factor is recommended to cover the laminar and turbulent flows as well as the influence of the surface finish. A weighted averaged model introduced by Aungier [16] can be used when the surface roughness becomes significant

$$(12) \quad Re_e = (Re - 2000)e/d > 60$$

Hence, the turbulent skin friction coefficient is defined as

$$(13) \quad c_f = c_{f_s} + (c_{f_r} - c_{f_s})(1 - 60/Re_e)$$

For a simple annular passage, hydraulic diameter can be assumed as the passage width, but for applying the generalized skin friction model to the compressor passage, the hydraulic diameter of the blade passage proposed by Jansen (equation 9) has been implemented into the weighted averaged model. In order to validate and examine the skin friction coefficient models, experimental data and unsteady CFD simulation over a wide range of operating conditions are needed.

2.2. NUMERICAL METHODS

To the best knowledge of the authors of this article, the only open access experimental data of a sCO₂ centrifugal compressor can be derived from the Sandia National laboratories reports [35], [36]. The studied case is the main centrifugal compressor in the Sandia split-flow re-compression sCO₂ Brayton cycle. The unshrouded impeller includes six main and six splitter blades, and the diffuser employs 17 wedge-shaped vanes. Main compressor dimensions are summarized in the table 2.

Table 2. Main compressor design dimensions [36].

Impeller diameter ratio d_2/d_{1h}	1.993
Impeller tip diameter	37.36 (mm)
Exit blade height	1.712 (mm)
Blade tip angle (minus is backswept)	-50 (deg)
Blade thickness	0.762 (mm)
Inlet blade angle at tip	50 (deg)
Normal tip clearance (constant)	0.254 (mm)
Exit vaned diffuser angle	71.5 (deg)

The mesh dependency test was previously done and by authors [23] and the total amount of around 1.5 million cells found to be sufficient since the compressor performance remained constant by increasing the number of cells. The sufficient fine cells near the walls were generated to ensure the values of y^+ close to unity. Figure 3 shows the Sandia centrifugal compressor geometry and structured mesh. The volute has not been modeled due to lack of geometrical data.

URANS equations were closed through the two equation $k - \omega$ SST turbulence model of Menter [37]. Convergence criteria of the CFD simulations were based on reduction of Root Mean Square (RMS) momentum, mass and energy residuals below 10⁻³%, reduction and stability of the imbalances of (difference between inlet and outlet in each zone) mass flow rate, energy and momentum below 10⁻²%, and the stability in the stage isentropic efficiency. Transient sliding mesh Blade Row interface employing the Fourier

Transformation was defined between the impeller and the vaned diffuser to capture the losses occurring in the transient situation as the flow is mixed between the rotating and stationary zones.

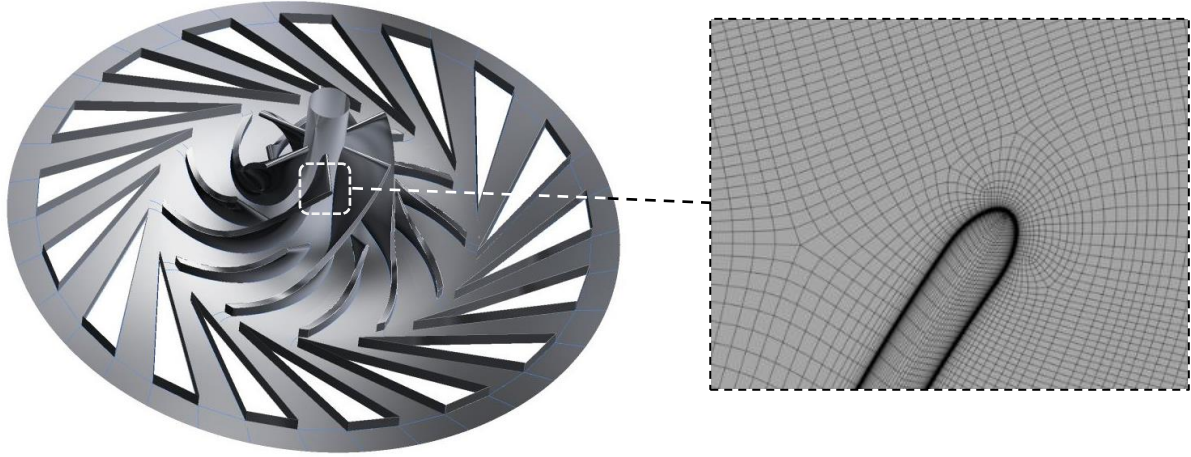


Figure 3. Geometry and mesh of the Sandia centrifugal compressor.

An external real gas properties (RGP) look-up table has been coupled with the flow solver. RGP table resolution is gradually increased by getting closer to the critical density curve and sufficiency wide range has been used to prevent clipping or extrapolating methods by the flow solver during the simulations. RGP dependency tests have been done by the present authors near the critical point and the optimum resolution of the table was also examined [23], [38]. Boundary conditions at the inlet are defined as total pressure and total temperature, reduced values (normalized with the critical value) are 1.042 and 1.006 for pressure and temperature, respectively. The static back pressure was set as the outlet boundary condition (reduced values are from 1.16 to 1.33 with interval size of 0.2 MPa). Skin friction coefficient can be calculated from the URANS simulations and is formulated as

$$(14) \quad c_f = \frac{\tau_w}{\frac{1}{2}\rho_\infty U_\infty^2}$$

where τ_w is the wall shear stress and U_∞ is the free-stream velocity. In the complicated geometries like inside the compressor flow passage, defining the free-stream velocity is not straightforward. A method introduced by Tiainen et al. [39] estimates the boundary layer thickness as a distance between the impeller blade and the location where the stream velocity is 99.5% of the adjacent point velocity as follows

$$(15) \quad \frac{dU}{dn} = 0.005$$

$$(16) \quad U_{n-1} = 0.995U_n$$

$$(17) \quad U_\infty = U_n$$

where the subscript n denotes normal to the wall. The same method is used in the present study to estimate the boundary layer thickness from hub to shroud direction as well to increase the accuracy of the numerical calculation. After locating the boundary layer thickness from each wall inside the impeller, values are averaged at different meridional distances and consequently the skin friction coefficient is calculated.

RESULTS AND DISCUSSION

Based on the different calculation methods, various values of skin friction loss are found. Figure 4 shows the skin friction coefficient distribution along the meridional distance of the studied impeller at the peak efficiency among the studied off-design points. Skin friction coefficient based on the CFD simulation fluctuates along the impeller passage from inlet to outlet. Normalized distances of 0.2 and 0.6 are the locations of the leading edges of the main and splitter blades, respectively. Higher values of skin friction coefficient can be noticed at the leading edges compared to adjustment points.

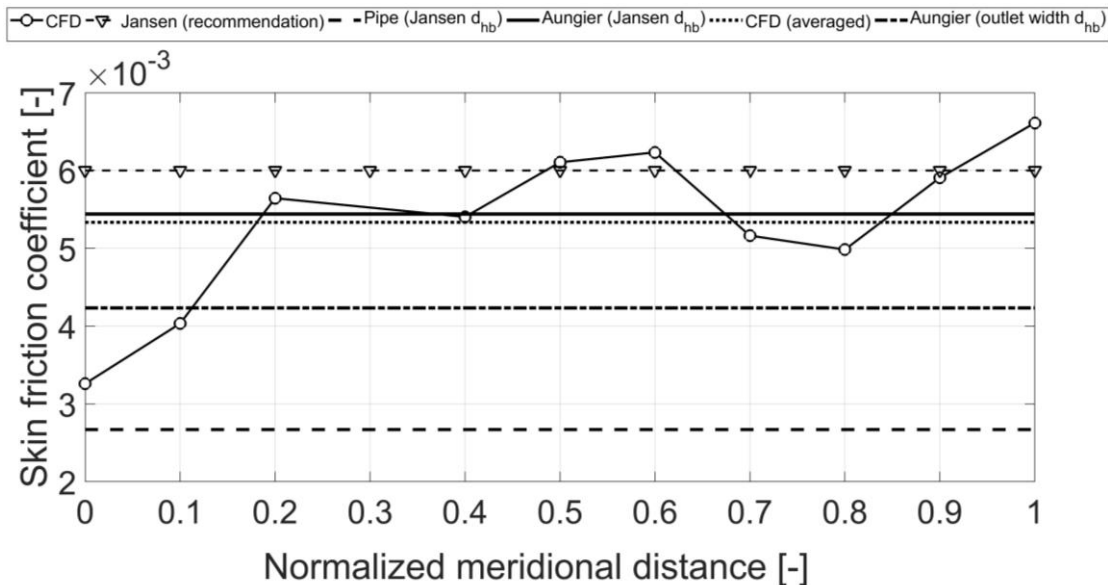


Figure 4. Comparison of skin friction coefficient.

To validate the performances of the meanline code and the CFD simulation, figure 5 shows their comparison against measurements for the compressor isentropic efficiency along the off-design points at 50 KRPM rotor speed (using the weighed averaged model of skin friction loss). Although, the CFD simulation overestimates the efficiency which results from neglecting the external loss effects, real gas numerical errors and geometrical deviations acceptable trend of CFD simulation and meanline code can be observed.

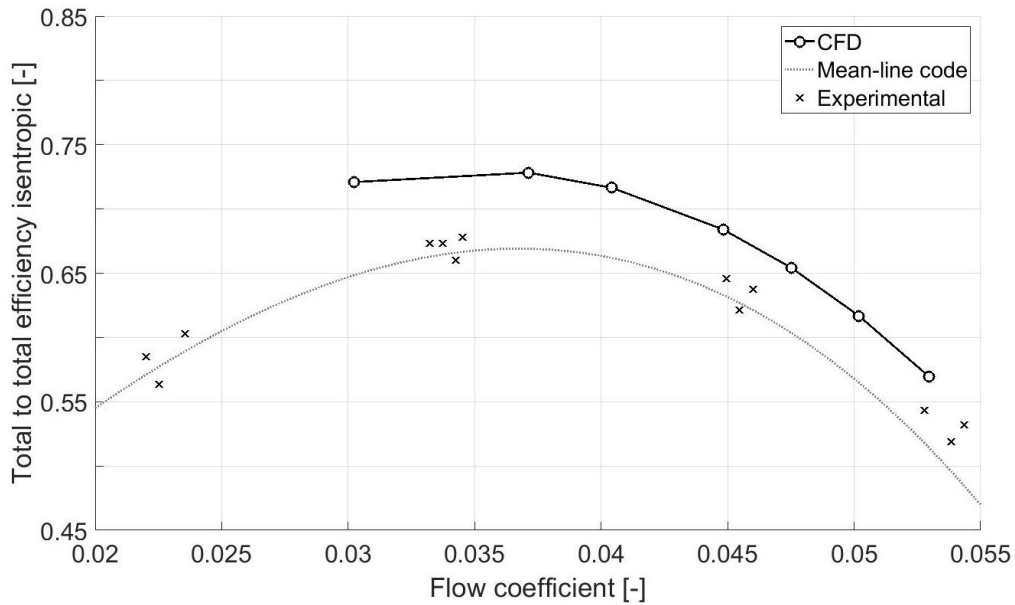


Figure 5. Map of the Sandia compressor at 50 KRPM.

The importance of skin friction loss can be highlighted by calculating the individual enthalpy loss models from table 1 at the design point. Figure 6 shows that the skin friction loss plays the most important role among all loss sources with share of more than 50 % of the total internal losses.

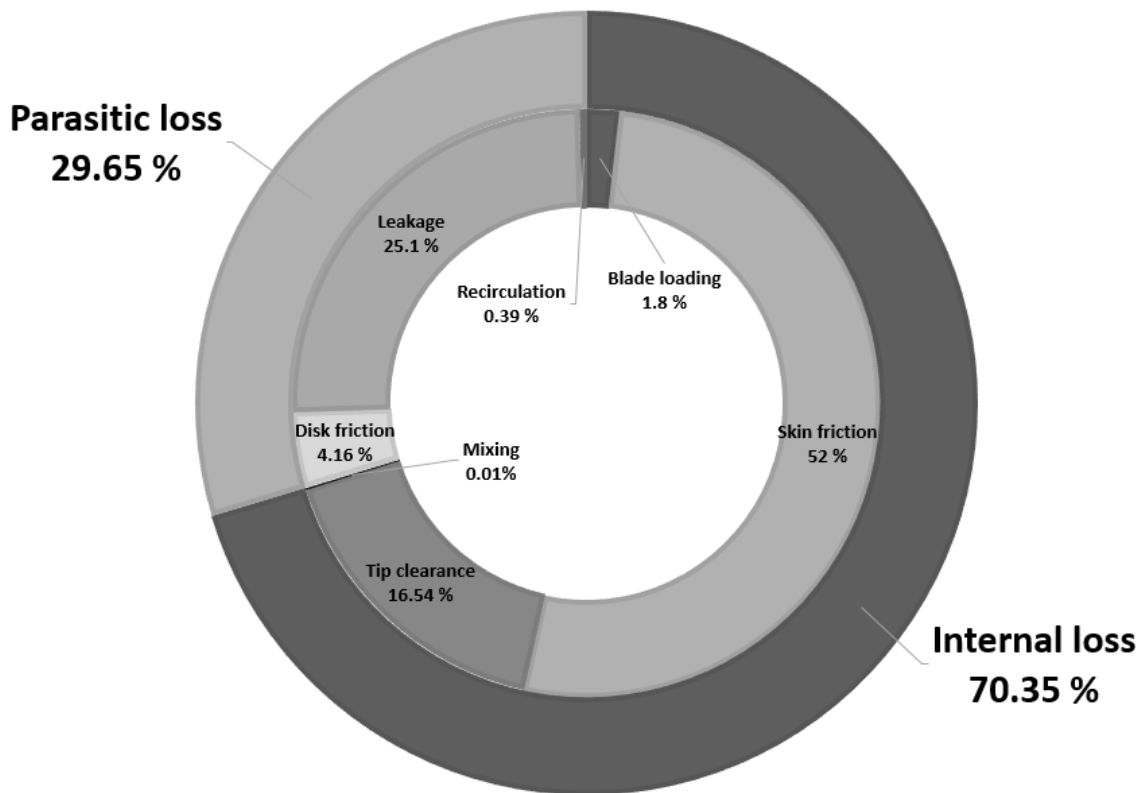


Figure 6. Share of the individual enthalpy loss.

As it can be seen, the friction loss is not constant along the impeller, and constant values may reduce the design accuracy. The model proposed by Jansen for pipe flows (equation 7) shows biggest difference against the CFD averaged value. While the weighted averaged model by Aungier (equation 13) combined with the hydraulic diameter assumption proposed by Jansen (equation 9) predicts the smallest difference. By implementing the hydraulic diameter value of Jansen in to the model proposed by Aungier, the difference is reduced but still around 81.8 % difference appears. The difference between CFD averaged value and the weighted averaged method is around 1.01 %.

CONCLUSION AND FUTURE WORK

Centrifugal compressor design based on the individual enthalpy loss models in the near critical point applications was investigated in this study. Due to small size of the compressor near the critical point (because of high density and low specific volume of fluid), skin friction loss was found to be the most significant and effective loss inside the rotor. Different models for skin friction coefficient were investigated and the result was compared against the URANS CFD simulation. A weighted averaged method proposed by Aungier by implementing the hydraulic diameter of the impeller passage by Jansen showed the best agreement with the CFD result. Also, by comparing the compressor map at constant rotor speed with the experimental measurement conducted at Sandia national lab, acceptable agreement between the meanline code, CFD simulation and measurement was achieved.

Throughout this process, it was clear that further investigation and improvement of the enthalpy loss models are needed. Also, more validation against experimental measurement should be done in order to confirm the presented method as a general statement. Moreover, compressor operates near the critical point and there is possibility of condensation around the suction side of the blades. Further studies are needed to apply the effect of condensation and its loss on the compressor performance and design.

ACKNOWLEDGEMENTS

The authors gratefully acknowledge the financial contribution of the Graduate School of Lappeenranta University of Technology.

REFERENCES

- [1] V. Dostal, "A Supercritical Carbon Dioxide Cycle for Next Generation Nuclear Reactors." pp. 1–317, 2004.
- [2] G. Angelino, "Carbon Dioxide Condensation Cycles for Power Production," *ASME J. Eng. Power*, vol. 90, no. 3, pp. 287–296, 1968.
- [3] A. Ameli, A. Afzalifar, T. Turunen-Saaresti, and J. Backman, "Effects of real gas model accuracy and operating conditions on supercritical CO₂ compressor performance and flow field," in *Proceedings of the ASME Turbo Expo*, 2017, vol. 9.

- [4] A. Ameli, T. Turunen-Saaresti, and J. Backman, "Numerical investigation of the flow behavior inside a supercritical CO₂ centrifugal compressor," in *Proceedings of the ASME Turbo Expo*, 2016, vol. 9.
- [5] A. Ameli, A. Afzalifar, and T. Turunen-Saaresti, "Non-equilibrium condensation of supercritical carbon dioxide in a converging-diverging nozzle," *J. Phys. Conf. Ser.*, vol. 821, no. 1, 2017.
- [6] S. G. Kim, "Uncertainty on performance measurement of S-CO₂ compressor operating near the critical point," pp. 1–9, 2014.
- [7] S. G. Kim, J. Lee, Y. Ahn, J. I. Lee, Y. Addad, and B. Ko, "CFD investigation of a centrifugal compressor derived from pump technology for supercritical carbon dioxide as a working fluid," *J. Supercrit. Fluids*, vol. 86, pp. 160–171, 2014.
- [8] C. Lettieri, N. Baltadjiev, M. Casey, and Z. Spakovszky, "Low-Flow-Coefficient Centrifugal Compressor Design for Supercritical CO₂," *J. Turbomach.*, vol. 136, no. 8, p. 81008, 2014.
- [9] T. Conboy, S. Wright, J. Pasch, D. Fleming, G. Rochau, and R. Fuller, "Performance Characteristics of an Operating Supercritical CO₂ Brayton Cycle," *J. Eng. Gas Turbines Power*, vol. 134, no. 11, p. 111703, 2012.
- [10] P. Garg, P. Kumar, and K. Srinivasan, "Supercritical carbon dioxide Brayton cycle for concentrated solar power," *J. Supercrit. Fluids*, vol. 76, pp. 54–60, 2013.
- [11] O. E. Balje, *Turbomachines-A guide to design, selection, and theory*. John Wiley & Sons, 1981.
- [12] J. Lee, J. I. Lee, H. J. Yoon, and J. E. Cha, "Supercritical Carbon Dioxide turbomachinery design for water-cooled Small Modular Reactor application," *Nucl. Eng. Des.*, vol. 270, pp. 76–89, 2014.
- [13] O. Conrad, K. Raif, and M. Wessels, "The calculation of performance maps for centrifugal compressors with vane-island diffusers," in *Performance prediction of centrifugal pumps and compressors*, 1979, pp. 135–147.
- [14] J. E. Coppage and F. Dallenbach, "Study of supersonic radial compressors for refrigeration and pressurization systems," 1956.
- [15] W. Jansen, "A method for calculating the flow in a centrifugal impeller when entropy gradients are present," in *Royal Society conference on internal aerodynamics (turbomachinery)*, 1967, pp. 133–146.
- [16] Ronald H. Aungier, *Centrifugal Compressors, A Strategy for Aerodynamic Design and Analysis*. ASME Press, 2000.
- [17] C. Rodgers, "Development of a High-Specific-Speed Centrifugal Compressor," *J. Turbomach.*, vol. 119, no. July, pp. 501–505, 1997.
- [18] H.-W. Oh, E. S. Yoon, and M. K. Chung, "An optimum set of loss models for performance prediction of centrifugal compressors," *Proc. Inst. Mech. Eng. Part A J. Power Energy*, vol. 211, no. 4, pp. 331–338, 1997.
- [19] A. Ameli, "AlFa CCD." 2017.
- [20] B. Kus and P. Nekså, "Development of one-dimensional model for initial design and evaluation of oil-free CO₂ turbo-compressor," *Int. J. Refrig.*, vol. 36, pp. 2079–2090, 2013.
- [21] E. W. Lemmon, M. L. Huber, and M. O. McLinden, "NIST Standard Reference Database 23: Reference Fluid Thermodynamic and Transport Properties-REFPROP, Version 9.1, National Institute of Standards and Technology." 2013.
- [22] R. Span and W. Wagner, "A new equation of state for carbon dioxide covering the fluid region from the triple-point temperature to 1100 K at pressures up to 800 MPa," *J. Phys. Chem. Ref. data*, vol. 25, no. 6, pp. 1509–1596, 1996.
- [23] A. Ameli, A. Afzalifar, T. Turunen-saaresti, and J. Backman, "EFFECTS OF REAL GAS MODEL ACCURACY AND OPERATING CONDITIONS ON SUPERCRITICAL CO₂ COMPRESSOR PERFORMANCE AND FLOW FIELD," in *Proceedings of ASME Turbo Expo 2017: Turbomachinery Technical Conference and Exposition*, 2017, pp. 1–10.
- [24] Y. Chen, P. Lundqvist, and P. Platell, "Theoretical research of carbon dioxide power cycle application in automobile industry to reduce vehicle's fuel consumption," *Appl. Therm. Eng.*, vol. 25, no. 14–15, pp. 2041–2053, 2005.
- [25] J. Sarkar, "Second law analysis of supercritical CO₂ recompression Brayton cycle," *Energy*, vol. 34, no. 9, pp. 1172–1178, 2009.
- [26] J. C. Wilkes and D. Ph, "Fundamentals of Supercritical CO₂," *ASME Turbo Expo 2014*, 2014.
- [27] N. D. (Nikola D. Baltadjiev, "An investigation of real gas effects in supercritical CO₂ compressors," 2012.
- [28] B. Monje, D. S??nchez, R. Chacartegui, T. S??nchez, M. Savill, and P. Pilidis, "Aerodynamic

- analysis of conical diffusers operating with air and supercritical carbon dioxide," *Int. J. Heat Fluid Flow*, vol. 44, pp. 542–553, 2013.
- [29] B. D. Iverson, T. M. Conboy, J. J. Pasch, and A. M. Kruiuzenga, "Supercritical CO₂ Brayton cycles for solar-thermal energy," *Appl. Energy*, vol. 111, pp. 957–970, 2013.
- [30] C. Lettieri, D. Yang, and Z. Spakovszky, "An Investigation of Condensation Effects in Supercritical Carbon Dioxide Compressors," *J. Eng. Gas Turbines Power*, vol. 137, no. 8, p. 82602, 2015.
- [31] M. H. Kim, J. Pettersen, and C. W. Bullard, *Fundamental process and system design issues in CO₂ vapor compression systems*, vol. 30, no. 2. 2004.
- [32] R. C. Johnston J. P. and Dean, "Losses in Vaneless Diffusers of Centrifugal Compressors and Pumps, Analysis, Experiment, and Design," *J. Eng. Power*, vol. 88, no. 1, 1966.
- [33] J. W. Daily and R. E. Nece, "Chamber Dimension Effects on Induced Flow and Frictional Resistance of Enclosed Rotating Disks," *J. Basic Eng.*, vol. 82, no. 1, pp. 217–230, Mar. 1960.
- [34] H. Schlichting, *Boundary-Layer Theory*. McGRAW-HILL, 1979.
- [35] S. A. Wright, T. M. Conboy, and G. E. Rochau, "Overview of supercritical CO₂ power cycle development at sandia national laboratories," *Univ. Turbine Syst. Res. Work.*, pp. 1–30, 2011.
- [36] S. A. Wright, R. F. Radel, M. E. Vernon, G. E. Rochau, and P. S. Pickard, "Operation and Analysis of a Supercritical CO₂ Brayton Cycle," no. September, pp. 1–101, 2010.
- [37] F. R. Menter, "Two-equation eddy-viscosity turbulence models for engineering applications," *AIAA J.*, vol. 32, no. 8, pp. 1598–1605, 1994.
- [38] A. Ameli, T. Turunen-saaresti, and J. Backman, "Numerical Investigation of the Flow Behavior Inside a Supercritical CO₂ Centrifugal Compressor," *ASME Turbo Expo 2016 Turbomach. Tech. Conf. Expo.*, 2016.
- [39] J. Tiainen, A. Jaatinen-Värri, A. Grönman, and J. Backman, "Effect of Free-Stream Velocity Definition on Boundary Layer Thickness and Losses in Centrifugal Compressors," in *ASME Turbo Expo 2017: Turbomachinery Technical Conference and Exposition*, 2017, p. Paper No. GT2017-63268.

Authors:



Alireza Ameli

Doctoral researcher and teacher assistant at Lappeenranta University of Technology, Finland. The main topic and interests are supercritical CO₂ thermophysical properties, turbomachinery and heat exchanger design. Eight research articles have been published/accepted in international journals and conferences since 2015.



Aki Grönman

He received his Doctor of Science (D.Sc.) degree from Lappeenranta University of Technology (LUT), Finland in 2010. He has been a visiting researcher at the Leibniz University of Hannover, Germany and University of Stuttgart, Germany. He is currently working as an associate professor at the School of Energy Systems at LUT, where his research interests include turbine and compressor aerodynamics and design with special interest in renewable energy production.



Teemu Turunen-Saaresti

He is Associate Professor (tenure track) at the School of Energy Systems at LUT. Generally, his research interests are related to energy conversion cycles and devices such as Organic Rankine Cycles (ORC), Supercritical Brayton Cycles, steam turbines, centrifugal compressors, and radial turbines.



Jari Backman

Dr. Jari Backman holds a position of professor in Applied Fluid Dynamics in Renewable Energy Systems. He has been managing various industrial projects within high-speed technology that has become commercial products. He has 35 years of experience in compressors, turbines, fans and pumps and has been involved in building and experimenting more than 30 prototypes.